Materials Science and Engineering C 58 (2016) 1199–1206

Contents lists available at ScienceDirect

Materials Science and Engineering C

journal homepage: www.elsevier.com/locate/msec

Photochemically modified diamond-like carbon surfaces for neural interfaces

A.P. Hopper [a], J.M. Dugan [a], A.A. Gill [a], E.M. Regan [b], J.W. Haycock [a], S. Kelly [c], P.W. May [b], F. Claeyssens [a,*]

[a] Department of Materials Science and Engineering, Kroto Research Institute, The University of Sheffield, Broad Lane, Sheffield S3 7HQ, UK
[b] School of Chemistry, University of Bristol, Bristol BS8 1TS, UK
[c] New Jersey Neuroscience Institute at JFK Medical Center, 65 James Street, Edison, NJ, USA

ARTICLE INFO

Article history:
Received 11 March 2015
Received in revised form 10 August 2015
Accepted 3 September 2015
Available online 8 September 2015

Keywords:
Diamond-like carbon
Neurons
Schwann cells
Amine
Aldehyde

ABSTRACT

Diamond-like carbon (DLC) was modified using a UV functionalization method to introduce surface-bound amine and aldehyde groups. The functionalization process rendered the DLC more hydrophilic and significantly increased the viability of neurons seeded to the surface. The amine functionalized DLC promoted adhesion of neurons and fostered neurite outgrowth to a degree indistinguishable from positive control substrates (glass coated with poly-L-lysine). The aldehyde-functionalized surfaces performed comparably to the amine functionalized surfaces and both additionally supported the adhesion and growth of primary rat Schwann cells. DLC has many properties that are desirable in biomaterials. With the UV functionalization method demonstrated here it may be possible to harness these properties for the development of implantable devices to interface with the nervous system.

1. Introduction

Diamond possesses a range of valuable mechanical and tribological properties, which offer interesting opportunities for the development of future applications. One such property, which is useful within biological research, is the ease with which it can be doped or functionalized whilst retaining its stability and biocompatibility [1]. Its mechanical strength and hardness are also particularly desirable especially where device longevity is a major concern. However, synthetic diamond is prepared under harsh conditions, usually requiring high temperatures and pressures, prohibiting its deposition upon biological or soft materials or upon common tissue culture substrates such as polystyrene or glass. In contrast diamond-like carbon (DLC), a form of amorphous carbon, has similar properties to diamond yet may be synthesised directly upon substrates under relatively mild deposition conditions and even at ambient temperature [2].

DLC films may be produced by a variety of methods including argon ion sputtering and cathodic arc spray or, as in this study, by pulsed laser deposition (PLD). The diamond-like character of the DLC produced is dependent upon the ratio of sp^2 and sp^3 carbon, with a higher sp^3 content resulting in more diamond-like properties. Importantly, both DLC and diamond may also be readily photo-functionalized with the aid of ultraviolet (UV) radiation allowing the attachment of a wide range of organic functional groups at the surface of the material [3]. Such an approach is ideal for modifying DLC for biomedical applications where the surface termination strongly affects protein and cell adhesion.

We have previously shown that photo-functionalized detonation nanodiamond is an effective mimic for poly-L-lysine (PLL), a synthetic adhesion factor commonly used in neural cell culture [4]. The neuroadhesive properties of PLL are thought to originate from the primary amine group on the side chain of the L-lysine residue, creating a highly polar molecule which assists in cell adhesion. Other molecules containing primary amines, such as 10-amino-dec-1-ene, are known to exert a similar neuroadhesive effect and may be covalently bound to DLC using the facile UV irradiation method.

In this study we have created a neurocompatible substrate from DLC, which possesses the positive attributes of conventional neuroadhesive surface treatments such as PLL. However, as the DLC is covalently functionalized, it is envisaged that the DLC substrates will exhibit lower cytotoxicity issues and greater stability in applications *in vivo*. This is the first time that covalently functionalized DLC has been evaluated as a growth substrate for neurons and Schwann cells. We anticipate that the techniques demonstrated here will find applications in surface coatings and device fabrication for the development of central nervous system implants such as electrodes for deep brain stimulation and in brain-computer-interfaces.

2. Materials and methods

Unless otherwise stated, all chemicals and bioreagents were obtained from Sigma-Aldrich (Dorset, UK) and used as received. Experimental

* Corresponding author.
E-mail address: f.claeyssens@sheffield.ac.uk (F. Claeyssens).

http://dx.doi.org/10.1016/j.msec.2015.09.013

samples were prepared and analysed in triplicate, unless otherwise stated, and error bars and statistical tests were calculated from these replicate measurements. Experiments were repeated at least once in order to ensure reproducibility. In all cases the presented micrographs were representative of the whole sample.

2.1. Preparation of diamond-like carbon substrates

In order to coat glass cover-slips with a thin coating of DLC, a pulsed laser deposition (PLD) method was used. The output of an argon fluoride (ArF) excimer laser (Lambda Physik, Compex 201) with a wavelength of 193 nm was focused (lens focal length: 200 mm, angle of incidence: 45°) on a graphite disc target (Poco Graphite Inc., DFP-3–2 grade) in a stainless steel chamber maintained at a pressure of approximately 10^{-6} Torr. The graphite was ablated using a laser fluence of 12 J/cm^2. A thin film of DLC of approximately 20 nm thickness was achieved with 1200 laser shots at a target-substrate distance of 5 cm at 20 °C. The DLC-treated cover-slips were then sonicated in methanol for 15 min and then washed in distilled water overnight. Once complete, the cover-slips were allowed to dry in air before being stored in an airtight container in preparation for use.

2.2. Synthesis of trifluoroacetate-protected 10-amino-dec-1-ene

Trifluoroacetate-protected 10-amino-dec-1-ene (TFAAD) was synthesised according to a method described elsewhere [3]. Firstly, 10-undecenoyl chloride (50.0 g, 0.25 mol) was added to tetrahexylammonium bromide (Acros Organics, Loughborough, UK, 0.6 mmol) in an ice bath. An aqueous solution of sodium azide (16.6 g in 50 ml) was then gradually added to the mixture within the ice bath and agitated using a magnetic stirrer. Once the reaction was complete, the organic fraction was separated, washed twice with deionised water, dried over anhydrous magnesium sulphate for 24 h and filtered. An excess of trifluoroacetic acid was then added to the acyl azide and the reaction mixture was heated to reflux under nitrogen for 6 h. The organic mixture was washed with a saturated solution of sodium bicarbonate, collected and subsequently dried over anhydrous magnesium sulphate for 24 h. The product was stored for later use at 4 °C.

2.3. Preparation of functionalized DLC

In order to ensure a uniform hydrogen-terminated surface, the glass cover-slips coated with DLC were hydrogenated by exposure to a hydrogen plasma flow for a total duration of 10 min prior to functionalization using the UV method. Hydrogenation was carried out in 2 cycles of 5 min with microwave power of 0.8 kW and 500 sccm H_2 total gas flow, followed by 2 min in cold H_2 flow under a pressure of 100 Torr. The coated cover-slips were then placed on top of a quartz slide, upon which a sufficient volume of either TFAAD (to prepare amine functional DLC) or undec-10-enal (to prepare aldehyde functional DLC) was applied to cover the samples. A further quartz slide was placed on top and the samples were exposed to UV radiation ($\lambda_{max} = 254$ nm) from a Hg–Xe lamp (500 W, Hamamatsu Photonics) for a period of 15 min in the case of undec-10-enal and 4 h in the case of TFAAD. Excess alkene was removed by rinsing in methanol. Where the alkene used was TFAAD, the protected amine was deprotected in acidified methanol (0.36 M HCl in methanol) at 65 °C over 24 h. The samples were washed in methanol, dried with a stream of nitrogen gas, and stored in sterile containers until required. For the sake of brevity the amine functional DLC will henceforth be designated "DLC-NH_2" and the aldehyde functional DLC will be designated "DLC-CHO".

2.4. X-ray photoelectron spectroscopy (XPS)

The surface chemistry of the functionalized samples was analysed using X-ray photoelectron spectroscopy (XPS). Samples were analysed using a Kratos AXIS Ultra DLD instrument. Spectra were recorded using a monochromatised Al Kα X-ray source (1486.6 eV) operating at a power of 150 W, whilst charging of the sample during irradiation was reduced by an internal flood gun. Each sample was analysed at an emission angle normal to the sample surface. Data processing, analysis and charge correction were carried out using CasaXPS software (ver.2.3.12 Casa Software Ltd.). Component peaks within the recorded C (1 s) spectra were deconvoluted and fitted to a mixed peak shape of 70% Gaussian/30% Lorentzian composition. The aliphatic hydrocarbon component of the C (1 s) was set to 285.0 eV as an internal reference.

2.5. Contact angle measurements

The relative hydrophobicity/hydrophilicity of the functionalized samples was determined by measuring the water contact angle. To ascertain the water contact angle of the DLC surfaces, one drop of deionised water (1 μl) was deposited on each surface. The contact angle was measured as the angle formed by the baseline and the tangent to the drop profile at the three-phase point using a Rame-Hart contact angle goniometer at a temperature of 21 °C. For each condition, four measurements were carried out on each of replicate samples, giving a total of 20 measurements for each condition ($n = 20$).

2.6. NG108-15 neuronal cell culture

NG108-15 neuronal cells were supplied by the American Type Culture Collection (ATCC). The cells were maintained and expanded in a growth medium comprising of Dulbecco's modified Eagle's medium (high glucose) supplemented with foetal bovine serum (10% *v*/*v*), L-glutamine (2 mM), penicillin (100 U/ml), streptomycin (100 μg/ml) and amphotericin B (0.25 μg/ml). Cells were not used experimentally beyond passage number 20. Neuronal cells were seeded upon DLC samples or glass coated with PLL at a density of 1×10^5 cells per ml in the complete growth medium without foetal bovine serum in order to induce terminal differentiation. The cells were cultured for 1, 2, 5 or 7 days at 37 °C and 5% CO_2 after which they were analysed for viability or fixed for microscopy as detailed in the following sections.

2.7. Isolation and culture of primary Schwann cells

Primary Schwann cells were isolated from male Wistar rats using the selective D-valine method reported elsewhere [5]. Animals were sacrificed in compliance with the Animals (Scientific Procedures) Act 1986. Briefly, sciatic nerves were removed from male Wistar rats (2–3 months) and the connective tissue was subsequently discarded. The nerves were teased and cut into 2–3 mm segments and incubated with 0.05% (*w*/*v*) collagenase (Sigma, UK) at 37 °C for 1 h. This cell suspension was then filtered through a 40 μm Falcon filter (Becton Dickinson, USA) and centrifuged at 400 RCF for 5 min. The resultant cell pellet was washed with DMEM (including 10% (*v*/*v*) foetal calf serum) and resuspended in Schwann cell growth medium containing DMEM-D-valine (PAA, UK), 2 mM glutamine, 10% (*v*/*v*) FCS, 1% (*v*/*v*) N2 supplement (Gibco BRL, UK), 20 μg/ml bovine pituitary extract, 5 μM forskolin (Sigma, UK), 100 U/ml penicillin, 100 μg/ml streptomycin and 0.25 μg/ml amphotericin B. The Schwann cell suspension was plated within 35 mm Petri dishes which had been previously coated with 0.5 mg poly-L-lysine/7 μg laminin (Sigma, UK). The cultures were maintained at 37 °C with 5% CO_2.

2.8. Identification of actin filaments and nuclei

At each time point the DMEM was removed from the NG108-15 neuronal cells, which were then washed once with phosphate buffered saline (PBS). To each well 500 μl of formalin (3.7% *v*/*v* in PBS) was applied for 15 min after which the cells were washed twice more with PBS. Cells were then permeabilised with Triton X-100 (0.1% *v*/*v* in PBS) for 5 min, before being washed two further times with PBS. A stock solution of

phalloidin-FITC (Sigma) was prepared at a concentration of 0.5 mg/ml in dimethyl sulfoxide (DMSO) and further diluted to a working concentration of 5 μg/ml in PBS. DAPI (Sigma) was added as a counterstain (final concentration of 10 μg/ml) and the combined stain solution was applied for 1 h at room temperature before the cells were rinsed three more times with PBS. Stained cells were visualised *via* fluorescence microscopy in PBS using a high throughput imaging and image analysis system (Image Xpress by Axon Instruments). Image analysis was carried out using the automated functionality of the imaging platform. The analysis process was conducted with oversight from the operator to ensure that erroneous measurements did not occur.

2.9. Immunofluorescent labelling of S100β

Immunofluorescent labelling was carried out to reveal S100β expression in Schwann cells cultured upon the functionalized DLC surfaces. S100β is a marker of the Schwann cell phenotype and continuous expression over time may indicate maintenance of the Schwann cell phenotype. After 21 days culture the medium was removed from the Schwann cell cultures, which were then washed once with PBS. The cells were then fixed with formalin (3.7% *v*/*v*) for 15 min, washed with PBS, and permeabilised with 0.1% Triton X-100 (Sigma-Aldrich, Dorset, UK) for 20 min at 4 °C. Cells were washed again with PBS and then blocked against non-specific antibody binding with 3% (*w*/*v*) bovine serum albumin (BSA) for 60 min at 4 °C. This was followed by incubation with polyclonal rabbit anti-S100β (1:250) (Dako) diluted in 1% (*w*/*v*) BSA overnight at 4 °C. The cells were washed twice with PBS and incubated with a FITC-conjugated secondary goat anti-rabbit IgG antibody (1:100 dilution in 1% (*w*/*v*) BSA) (Vector Labs, USA) for 90 min at room temperature.

2.10. Viability assay (MTT)

Relative cell viability plus an indication of rate of proliferation was assessed indirectly by the MTT assay. Cells were cultured on three samples for each condition ($n = 3$) at a density of 10,000 cells/ml within 24 well plates (Costar) over periods of 1, 2, 5 and 7 days. At each time point the DMEM was removed from selected wells and the cells were washed once with PBS. MTT Solution (thiazolyl blue tetrazolium bromide, Sigma) was dissolved in PBS (0.5 mg/ml) and 300 μl was added to each well. The cells were incubated at 37 °C and 5% CO_2 for 45 min after which the MTT solution was removed and the reduced product was solubilised in 300 μl acidified isopropanol (1.25 μl HCL (37% *w*/*w*) per ml of isopropanol). The resulting solution was transferred in triplicate 100 μl volumes to a 96-well plate where the optical density was measured at 540 nm relative to 630 nm.

3. Results

3.1. Surface functionalization and characterisation of DLC

DLC was applied to the surface of glass cover-slips *via* pulsed laser deposition. The DLC-coated glass was then subjected to UV-induced functionalization with TFAAD or undec-10-enal to yield either amine (after deprotection) or aldehyde-functionalized substrates. Contact angle measurements were carried out to provide an initial indication of the success of the functionalization process and to provide insight into the hydrophobicity of the samples, which may have implications for subsequent cell culture studies. The contact angle of a surface describes its wettability. Smaller contact angles, namely those below 90°, characterise hydrophilic surfaces which are highly wettable, whereas large contact angles correspond to hydrophobic surfaces which exhibit reduced wettability.

Contact angle measurements on the pristine DLC and functionalized DLC surfaces are shown in Fig. 1. The contact angle of glass (52.1° ± 4.8°) was also measured as a comparison. Compared to glass, which is regarded as a relatively hydrophilic material, the pristine DLC was more hydrophobic with a higher contact angle (64.3° ± 3.1°). Upon functionalization, however, the contact angle decreased on both the DLC-NH_2 (48.4° ± 1.7°) and DLC-CHO (49.7° ± 2.9°) surfaces. The functionalized surfaces were significantly more hydrophilic than the pristine DLC with contact angles comparable to glass.

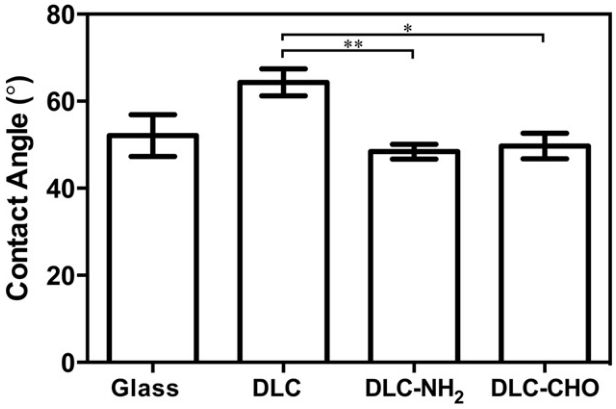

Fig. 1. Contact angle of water on glass, pristine DLC, DLC-NH_2 and DLC-CHO. Values are reported as the mean ± standard error. Statistical significance was determined by one-way ANOVA followed by Tukey's multiple comparison test; * = $p < 0.05$ and ** = $p < 0.01$.

The functionalized DLC samples were further characterised by XPS to reveal the composition of their surface chemistry. High-resolution spectra of the C 1 s region are shown in Fig. 2. Because carbon bound to fluorine gives rise to a distinct chemical shift in the C 1 s peak, the DLC-NH_2 samples were analysed prior to removal of the trifluoroacetate protecting group in order to aid in confirmation of successful functionalization. In each case the C 1 s peak was deconvoluted into component peaks arising from the different chemical environments of carbon in the first few nanometres depth of the material, including any modification of the surface chemistry. The percentage of the total C 1 s attributable to each component peak is given in the supplementary information, accessible online.

In each of the spectra in Fig. 2 the C 1 s peak is dominated by the component at 285 eV corresponding to carbon in an aliphatic hydrocarbon environment or an equivalent environment without heteroatoms (*e.g.* DLC). In addition, several components form a shoulder at higher binding energies in each spectrum. In pristine DLC (Fig. 2a) these components collectively contribute to just over 8% of the total C 1 s peak area and arise from the native oxide layer on the surface of the material. For the functionalized samples, however, the components forming the shoulder correspond to the surface layer arising from the UV functionalization in addition to any native oxide layer on the DLC. On the DLC-NH_2 sample the components at higher binding energy than the aliphatic component account for just under 22% of the total C 1 s peak area, with significantly larger peaks centred at 286.32 eV and 288.94 eV corresponding to carbon singly bound to nitrogen (or oxygen) and carbonyl-containing groups respectively. In addition, a new peak centred at 293.17 eV corresponding to carbon bound to fluorine was observed, in contrast to the pristine DLC or DLC-CHO samples, confirming successful binding of the trifluoroacetate-protected amine. On the DLC-CHO samples, just over a two-fold increase in the area of the peak centred at 286.31 eV and a four-fold increase in the area of the peak centred at 288.94 eV was observed relative to the pristine DLC. Respectively, these peaks likely correspond to carbon singly bound to a heteroatom (*e.g.* alcohol or ether functionalities) and a carbonyl group bound to an additional heteroatom (*e.g.* ester, amide or carboxylic acid). Although it is clear that successful addition of an organic layer had taken place in these samples, from the spectra it seems likely that some oxidation of the aldehyde functionality occurred during the UV functionalization process.

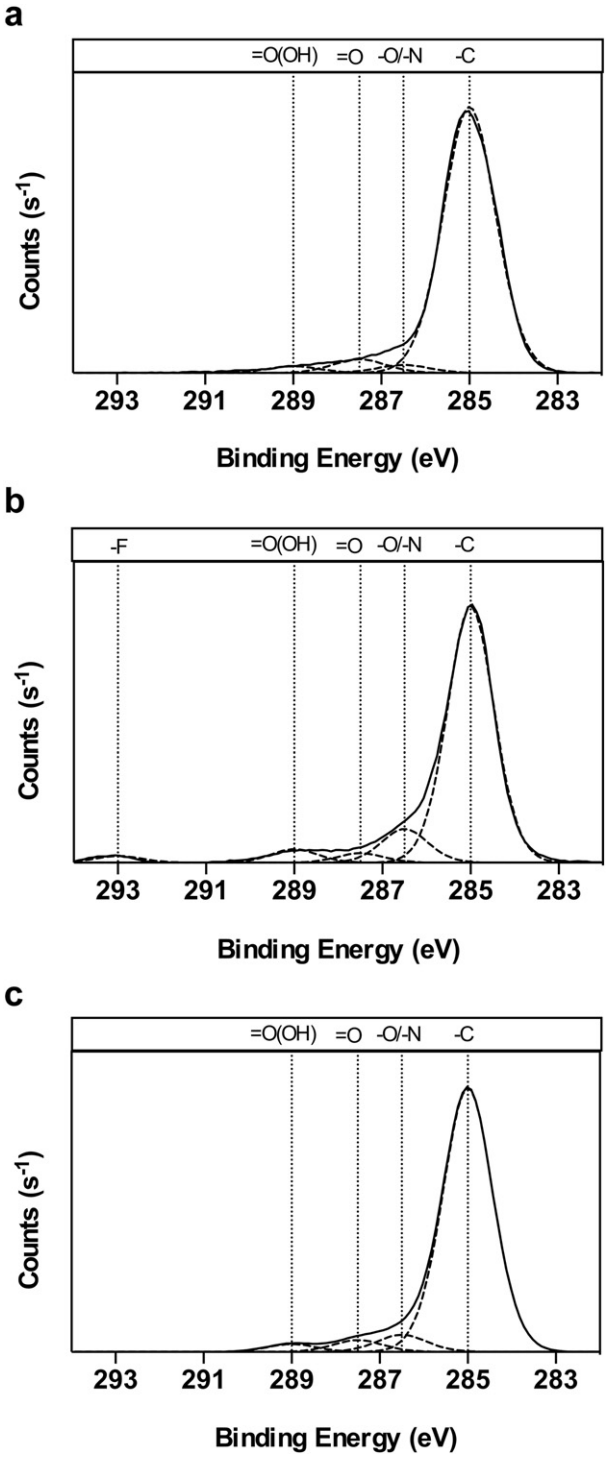

Fig. 2. Carbon 1 s region high-resolution XPS spectra of functionalized DLC samples. (a) Pristine DLC. (b) DLC-NH_2 (prior to deprotection). (c) DLC-CHO. In each case the C 1 s peak was deconvoluted into component peaks corresponding to the different chemical environments of C on the sample surfaces (dashed lines). Characteristic binding energies of the functional groups corresponding to the component peaks are labelled and marked with dotted lines.

3.2. Neuronal cell culture on functionalized DLC surfaces

3.2.1. Cell viability

To provide an indication of neuronal cell adhesion and viability upon the functionalized surfaces, an MTT assay was performed 7 days post cell-seeding on the pristine DLC, DLC-NH_2 and DLC-CHO surfaces plus uncoated glass as a negative control and glass coated with PLL as a positive control (Fig. 3). Statistically significant differences were observed between certain samples. The summary of the statistical analysis is given in Table 1.

MTT absorbance values were comparatively low on both the glass (negative control) and the pristine DLC, indicating a low level of viable neuronal cell attachment and accompanying low levels of cell proliferation. In contrast, on both the functionalized DLC surfaces relatively high MTT absorbance values were observed, comparable to the PLL (positive control) surfaces. For example the value for DLC-NH_2 (0.87) was over 4 times higher than the corresponding reading from pristine DLC (0.17). Although cells grown upon PLL gave a slightly higher average reading (0.97) than those grown upon DLC-NH_2 surfaces, there was no statistical difference between the two conditions. The reading from cells grown upon the DLC-CHO surfaces was also significantly higher than on the glass and pristine DLC, although statistically lower than on the PLL and DLC-NH_2 surfaces.

3.2.2. Differentiation of NG108-15 neuronal cells

NG108-15 neuronal cells were allowed to terminally differentiate upon pristine DLC, DLC-CHO and DLC-NH_2 surfaces. In addition, uncoated glass and glass coated PLL were used as negative and positive controls respectively. The cells were cultured for 7 days, after which they were stained with FITC-conjugated phalloidin to reveal filamentous actin and hence their cytoskeletal morphology. Fluorescence micrographs are shown in Fig. 4.

Although cells adhered to all the surfaces tested, comparatively few were observed on glass (Fig. 4a) or pristine DLC (Fig. 4c). Cells on these surfaces displayed few dendrites and those that had developed were considerably shorter than on the other surfaces. The cells adopted a spherical morphology with little spreading and minimal contact area with the substrate. A much greater degree of cell adhesion was observed on the PLL surfaces (Fig. 4b) as well as upon the functionalized DLC surfaces (Fig. 4d and e). The cells were cultured in the absence of serum or mitogens in order to promote terminal differentiation so a significant degree of proliferation was unlikely. The differences in cell density are therefore likely due to differences in initial adhesion given that cells were seeded at the same concentration on all samples. Significant numbers of much longer dendrites were also observed on the PLL and functionalized DLC surfaces and numerous cells displayed a bipolar or even tripolar morphology, some possessing dendrites with lengths exceeding 300 μm. Upon the DLC-NH_2 surfaces especially, cells appeared to adhere and develop similarly to those cultured upon PLL resulting in almost identical morphology and degree of confluence.

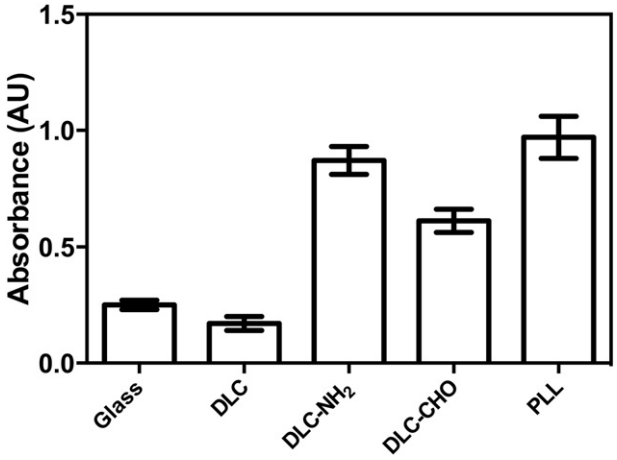

Fig. 3. MTT assay absorbance values, measured at 570 nm and referenced at 630 nm, for NG108-15 neuronal cells cultured upon glass, pristine DLC, DLC-NH_2, DLC-CHO and PLL surfaces over a period of 7 days. Values are reported as mean ± standard error.

Table 1
Summary of statistical analysis of MTT assay results shown in Fig. 3. Statistical analysis was carried out by one-way ANOVA followed by Tukey's multiple comparison test. * = $p < 0.05$, ** = $p < 0.01$, *** = $p < 0.001$ and N/S = no significant difference.

	DLC	DLC-CHO	DLC-NH_2	PLL
Glass	N/S	***	***	***
DLC		***	***	***
DLC-CHO			*	***
DLC-NH_2				N/S

Automated image analysis of the fluorescence micrographs was also carried out in order to quantify the dendricity of the cells at various time points to give an indication of the degree of terminal differentiation and the suitability of the different surfaces to support outgrowth of neurites. Graphs summarising the mean number of neurites per cell and average neurite length are shown in Fig. 5a and b respectively. Full statistical analysis was also carried out and the results are given in the supplementary information which is available online.

In terms of mean number of neurites per cell, two trends were observed. On the glass and pristine DLC samples a moderate increase in the number of dendrites was observed over time followed by a decrease in neurite number culminating in almost complete absence of neurites by day 7. In contrast, on the PLL surfaces and the functionalized DLC surfaces, a steady increase in the number of neurites per cell was observed over time. By day 7 the largest number of neurites per cell was observed on the DLC-NH_2 surfaces, a difference which was statistically significant in comparison with the PLL and DLC-CHO surfaces ($p < 0.01$). No statistically significant difference was observed between the DLC-CHO surfaces and PLL.

Similar trends were also observed in the average neurite length (Fig. 5b). A steady decrease in neurite length was observed over time on both the glass and pristine DLC surfaces. Although neurite length appeared slightly greater on DLC compared to glass at all time points, the observed difference was not statistically significant except at day 2 ($p < 0.01$). In contrast, the average neurite length increased steadily over time on the functionalized DLC and PLL samples. By day 7 there was no statistically significant difference between the DLC-NH_2 samples and the PLL positive controls. Neurite length was slightly lower on the DLC-CHO samples compared to the DLC-NH_2 and PLL samples, although this difference was statistically significant only in comparison with PLL ($p < 0.001$).

3.2.3. Primary Schwann cell culture

Primary Schwann cells were cultured upon glass, pristine DLC, DLC-NH_2 and PLL surfaces for 21 days after which they were stained for the glial marker S100β. Fluorescence micrographs are shown in Fig. 6.

Clear differences in Schwann cell morphology were observed across the different surfaces. In contrast to the NG108-15 neuronal cells, a considerable number of Schwann cells attached to the glass substrate (Fig. 6a). On glass the cell morphology was either bipolar or tripolar with thin processes that showed no particular orientational preference. A small degree of Schwann cell attachment was also observed on the pristine DLC surfaces (Fig. 6c). However, in contrast to cells on the glass surfaces, the cells on pristine DLC adopted a variety of uncharacteristic morphologies, some resembling fibroblasts whilst others adopted a highly spread polygonal morphology. Nonetheless, positive expression of the glial marker S100β was still observed on both the glass and pristine DLC surfaces.

In contrast to those on glass and pristine DLC, Schwann cells cultured upon DLC-NH_2 and PLL surfaces formed confluent monolayers and exhibited similar morphologies. The cells adopted a bipolar, elongated morphology, which is characteristic of Schwann cells, and nearly all processes were aligned alongside adjacent cells. The confluent cell monolayers appeared stable and showed no sign of delamination from the substrate.

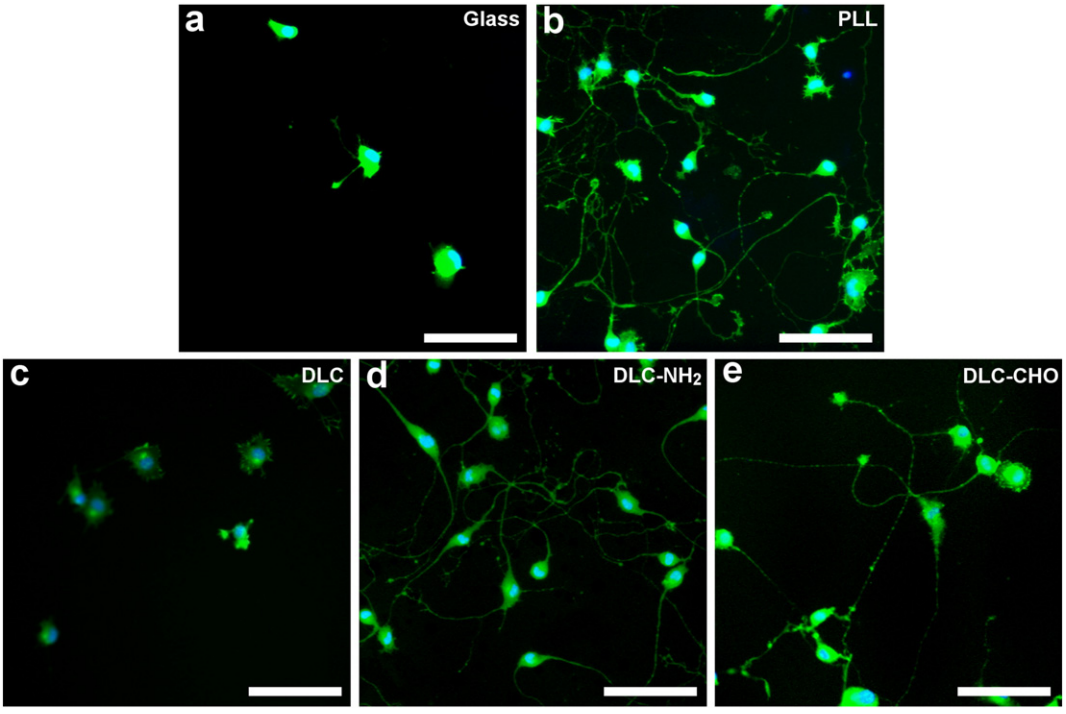

Fig. 4. Fluorescence micrographs of NG108-15 neuronal cells cultured for 7 days. (a) Glass (negative control). (b) PLL (positive control). (c) DLC. (d) DLC-NH_2. (e) DLC-CHO. Cells were stained for F-actin with FITC-labelled phalloidin (green) and counterstained for nuclei with DAPI (blue). Scale bars: 100 μm.

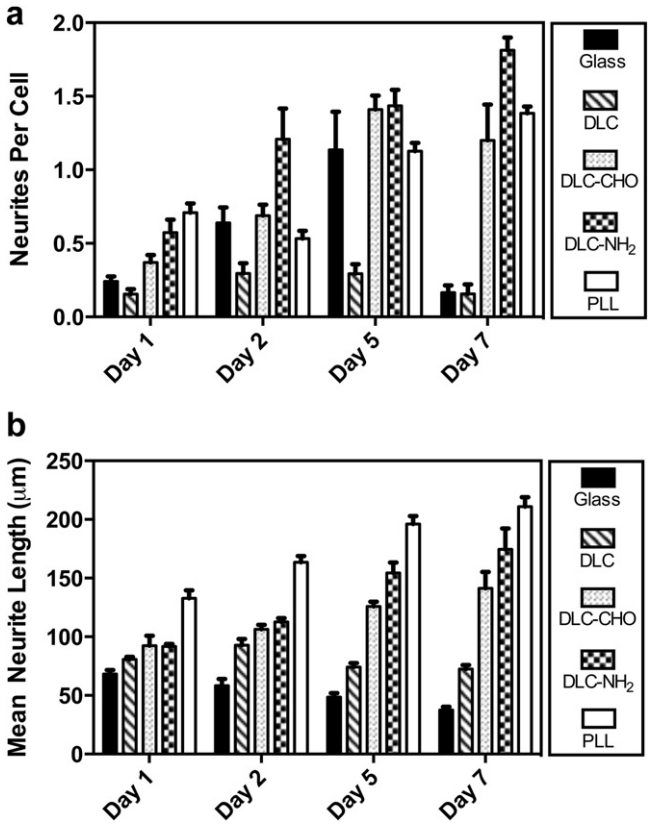

Fig. 5. Image analysis of NG108-15 neuronal cell dendricity from fluorescence micrographs of cells growing upon glass, DLC, DLC-CHO, DLC-NH_2 and PLL surfaces after 1, 2, 5 and 7 days. Values are reported as the mean of three replicate samples ± standard error. (a) Mean number of neurites per cell. (b) Mean neurite length. Full statistical analysis was carried out, the results of which are given in the supplementary information.

4. Discussion

We have prepared DLC substrates which were subsequently modified by a UV functionalization method to covalently bond amine and aldehyde-containing molecules to the surface in order to improve neurocompatibility. DLC and related materials, such as CVD diamond, have several interesting properties which support their use as biomaterials. Firstly they may be readily doped or functionalized to alter their bulk characteristics, for example electrical properties, to suit the desired application [2,6–10]. Diamond-based materials have also been tested exhaustively to prove their biocompatibility and low toxicity [11–16]. With respect to manufacturing, DLC is also advantageous in that the size or shape of objects to be coated is of little consequence to the coating procedure. Most components and devices may be treated swiftly and at relatively low expense to create a stable and robust surface layer [2,17]. Additionally, although of less relevance in neurosurgical applications, the wear-resistance of DLC could provide comparatively high longevity for any potential implants, potentially reducing the need for revision surgery in certain applications [2].

Hydrogen-terminated diamond-like materials, such as the DLC produced by pulsed laser deposition used in this study, are known to inhibit neuronal growth due to the lack of adequate interaction sites to facilitate cell adhesion [18]. By suitable surface modification, however, biocompatibility and bioactivity may be significantly improved. Upon modification with surface-bound amine and aldehyde groups DLC was shown to promote adhesion of NG108-15 neuronal cells and primary rat Schwann cells. Furthermore, the NG108-15 neuronal cells produced long neurites and in the case of the amine functional DLC were indistinguishable from the positive control coating (PLL).

Although there are several variables that dictate the survival, growth and differentiation of neuronal cells *in vitro*, one of the most important is the culture substrate [19,20]. Substrates that have been widely used in the culture of neuronal cells include glass and tissue culture plastic that have been coated with attachment factors of some kind. The most common attachment factors are cationic polypeptides of basic amino acids such as poly-L-lysine (PLL) and poly-L-ornithine [21,22], whilst extracellular matrix components including laminin have also been applied, with collagen and fibronectin also being used to a lesser extent [23–26]. Such coatings have become widespread as a pre-treatment for neuronal cell culture since they promote cellular adhesion, survival and neurite outgrowth [19,20,22,27].

It is not entirely clear how substances such as PLL, which contain amine groups, improve cell attachment and viability. The effect may arise from interactions with specific receptors on neuronal cell membranes enhancing adhesion to the substrate. Alternatively, a cationic polypeptide may act as a positively charged interlayer, electrostatically binding the negatively charged cell membrane to the substrate surface [22,28,29]. Proteins originating from the serum component of the cell medium have also been identified as assisting cell adhesion, acting in a similar manner to extracellular matrix proteins [29]. Substrates coated with PLL have been shown to lead to the development of a greater thickness of adsorbed proteins during cell culture compared to control surfaces, these either being secreted by the cells or adsorbed from the constituents of the culture medium [20]. Proteins which adsorb initially to PLL undergo denaturation and do not encourage neuronal adhesion; however subsequent proteins which bind to this denatured layer retain their structure intact, thus encouraging subsequent cell adhesion.

Although PLL is often used as the standard attachment factor to support the growth of Schwann cells *in vitro*, it is not envisaged to be desirable or permissible to use such synthetic polypeptides for *in vivo* applications such as neural prosthetics due to concerns about toxicity [30]. Covalent functionalization of culture substrates is therefore an appealing alternative in developing such applications. It has previously been demonstrated that surface-bound amine groups can support neuronal adhesion and differentiation similarly without detrimental effects [31]. Although research in this area is ongoing it is thought that amines interact with cells through membrane-bound chondroitin sulphate proteoglycans (CSPGs). These proteoglycans exert significant influence over neuronal differentiation *via* integrin-mediated signalling which may explain the neurocompatibility of amines and amine-containing substances such as PLL [32,33].

It is possible that by covalently functionalizing surfaces with amine groups the longevity of the neurocompatibility may be enhanced in comparison to PLL. Indeed it has been shown that significantly higher shear stresses were required to detach NG108-15 cells from covalently-modified amine surfaces, in comparison to those functionalized with ECM proteins [19]. This was corroborated by further research which concluded that covalently bound PLL was far more effective at retaining adhered cells than PLL that was passively adsorbed to the substrate [22]. An additional benefit of covalently bound functionalities is their lack of leaching into solution, contrasting with non-covalently bound PLL the gradual desorption of which can result in cell dissociation [22]. All these factors demonstrate the advantages of the UV functionalization approach demonstrated here.

In addition to amine groups, aldehyde groups were also introduced to the surface of the DLC using a similar UV functionalization method (with undec-10-enal). In the cell culture studies the aldehyde functional group performed broadly comparably to the amine group with similar levels of neuronal viability, attachment and neurite development and indistinguishable Schwann cell attachment and morphology. Although relatively little research has been undertaken regarding such aldehyde-containing functionalities for cell growth, aldehyde terminated surfaces are regarded as being hydrophilic. In addition, plasma polymerised surfaces formed from aldehyde-containing monomers have been shown to support the growth and attachment of cells to a

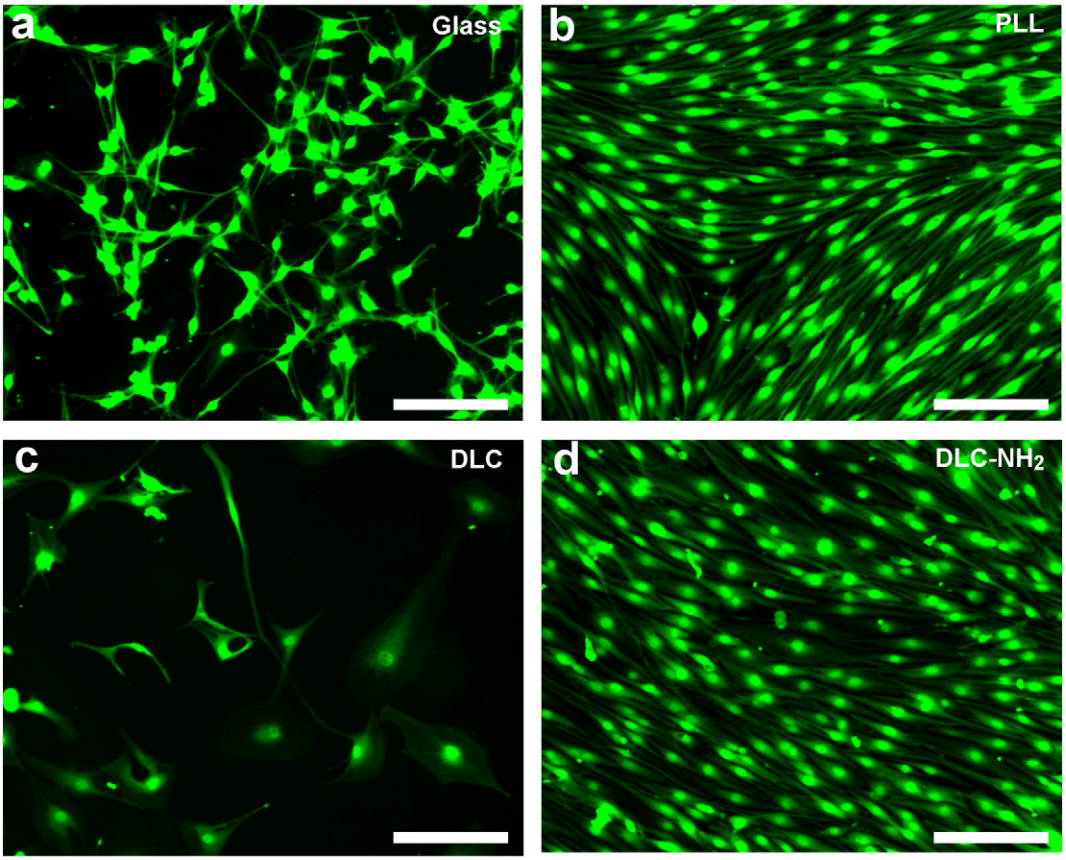

Fig. 6. Fluorescence micrographs of primary rat Schwann cells cultured for 21 days. (a) Glass. (b) PLL. (c) Pristine DLC. (d) DLC-NH_2. Cells were immunolabelled for S100β. Scale bars: 100 μm.

similar degree as those cultured upon tissue culture modified polystyrene [34].

Aldehyde-functionalized substrates have been shown to be capable of immobilising proteins upon their surface to produce self-assembled monolayers (SAMs) of protein, indicating that they may be used for applications within the biosensor research field as well as for direct interface with cell and tissues [35]. A similar study has also shown that surfaces bearing aldehyde groups may immobilise proteins from solution (in this case bFGF) which may then act as ligands for specific receptors allowing the capture and adhesion of cells [36]. It seems highly likely that a similar mechanism could occur in which serum proteins such as fibronectin could be captured by surface-bound aldehydes, leading to increased cell adhesion. As it is known that adhesion receptors within the cell membrane not only influence the adherence of cells but also mediate cellular growth and differentiation, the importance of engineering substrates that promote cellular adhesion is clear [37,38]. Although the DLC-CHO surfaces supported neuron and Schwann cell adhesion and differentiation of NG108 cells, by some measures (neurite length and viability) these surfaces did not perform as well as the amine-bearing surfaces. The reason for this is not clear but may be due to differences in both the degree of protein adsorption and the conformation of adsorbed proteins. Elucidation of this mechanism would require further study.

5. Conclusions

The surface of DLC was modified using a UV functionalization method to introduce amine and aldehyde groups to improve neurocompatibility. The functionalization process rendered the DLC more hydrophilic and significantly increased the viability of neuron-like cells seeded to the surfaces. The amine-functionalized DLC promoted neuron adhesion and neurite outgrowth to a degree indistinguishable from positive control substrates. The aldehyde-functionalized surfaces performed comparably to the amine-functionalized surfaces and both additionally supported the adhesion and growth of primary rat Schwann cells. With the UV functionalization method demonstrated here it may be possible to harness the unique properties of DLC for the development of implantable devices to interface with the nervous system.

Acknowledgements

The authors are grateful to EPSRC for funding this work in the form of a studentship for AH and PDRA position for JD supported under grant number EP/K002503/1. The Sheffield Surface Analysis Centre and Kroto Imaging Facility are also gratefully acknowledged.

Appendix A. Supplementary data

Supplementary data to this article can be found online at http://dx.doi.org/10.1016/j.msec.2015.09.013.

References

[1] P.W. May, E.M. Regan, A. Taylor, J. Uney, A.D. Dick, J. McGeehan, Spatially controlling neuronal adhesion on cvd diamond, Diam. Relat. Mater. 23 (2012) 100–104.
[2] E.M. Regan, J.B. Uney, A.D. Dick, Y.W. Zhang, J. Nunez-Yanez, J.P. McGeehan, F. Claeyssens, S. Kelly, Differential patterning of neuronal, glial and neural progenitor cells on phosphorus-doped and UV irradiated diamond-like carbon, Biomaterials 31 (2) (2010) 207–215.
[3] B. Sun, P.E. Colavita, H. Kim, M. Lockett, M.S. Marcus, L.M. Smith, R.J. Hamers, Covalent photochemical functionalization of amorphous carbon thin films for integrated real-time biosensing, Langmuir 22 (23) (2006) 9598–9605.
[4] A.P. Hopper, J.M. Dugan, A.A. Gill, O.J.L. Fox, P.W. May, J.W. Haycock, F. Claeyssens, Amine functionalized nanodiamond promotes cellular adhesion, proliferation and neurite outgrowth, Biomed. Mater. **9** (4) (2014).

[5] R. Kaewkhaw, A.M. Scutt, J.W. Haycock, Integrated culture and purification of rat Schwann cells from freshly isolated adult tissue, Nat. Protoc. 7 (11) (2012) 1996–2004.
[6] S. Neuville, A. Matthews, A perspective on the optimisation of hard carbon and related coatings for engineering applications, Thin Solid Films 515 (17) (2007) 6619–6653.
[7] T.C. Kuo, R.L. McCreery, G.M. Swain, Electrochemical modification of boron-doped chemical vapor deposited diamond surfaces with covalently bonded monolayers, Electrochem. Solid-State Lett. 2 (6) (1999) 288–290.
[8] S.C.H. Kwok, W. Jin, P.K. Chu, Surface energy, wettability, and blood compatibility phosphorus doped diamond-like carbon films, Diam. Relat. Mater. 14 (1) (2005) 78–85.
[9] S.C.H. Kwok, P.C.T. Ha, D.R. McKenzie, M.M.M. Bilek, P.K. Chu, Biocompatibility of calcium and phosphorus doped diamond-like carbon thin films synthesized by plasma immersion ion implantation and deposition, Diam. Relat. Mater. 15 (4–8) (2006) 893–897.
[10] N. Yang, H. Uetsuka, H. Watanabe, T. Nakamura, C.E. Nebel, Photochemical attachment of amine-layers on h-terminated undoped single crystalline cvd diamonds, Diam. Relat. Mater. 17 (7–10) (2008) 1376–1379.
[11] S.J. Yu, M.W. Kang, H.C. Chang, K.M. Chen, Y.C. Yu, Bright fluorescent nanodiamonds: no photobleaching and low cytotoxicity, J. Am. Chem. Soc. 127 (50) (2005) 17604–17605.
[12] K.K. Liu, C.L. Cheng, C.C. Chang, J.I. Chao, Biocompatible and detectable carboxylated nanodiamond on human cell, Nanotechnology **18** (32) (2007).
[13] A.M. Schrand, L. Dai, J.J. Schlager, S.M. Hussain, E. Osawa, Differential biocompatibility of carbon nanotubes and nanodiamonds, Diam. Relat. Mater. 16 (12) (2007) 2118–2123.
[14] W.J. Ma, A.J. Ruys, R.S. Mason, P.J. Martin, A. Bendavid, Z.W. Liu, M. Ionescu, H. Zreiqat, Dlc coatings: Effects of physical and chemical properties on biological response, Biomaterials 28 (9) (2007) 1620–1628.
[15] C. Hinuber, C. Kleemann, R.J. Friederichs, L. Haubold, H.J. Scheibe, T. Schuelke, C. Boehlert, M.J. Baumann, Biocompatibility and mechanical properties of diamond-like coatings on cobalt–chromium–molybdenum steel and titanium–aluminum–vanadium biomedical alloys, J. Biomed. Mater. Res. Part A 95A (2) (2010) 388–400.
[16] N. Mohan, C.-S. Chen, H.-H. Hsieh, Y.-C. Wu, H.-C. Chang, In vivo imaging and toxicity assessments of fluorescent nanodiamonds in *Caenorhabditis elegans*, Nano Lett. 10 (9) (2010) 3692–3699.
[17] S. Kelly, E.M. Regan, J.B. Uney, A.D. Dick, J.P. McGeehan, E.J. Mayer, F. Claeyssens, G. Bristol Biochip, Patterned growth of neuronal cells on modified diamond-like carbon substrates, Biomaterials 29 (17) (2008) 2573–2580.
[18] T. Lechleitner, F. Klauser, T. Seppi, J. Lechner, P. Jennings, P. Perco, B. Mayer, D. Steinmuller-Nethl, J. Preiner, P. Hinterdorfer, M. Hermann, E. Bertel, K. Pfaller, W. Pfaller, The surface properties of nanocrystalline diamond and nanoparticulate diamond powder and their suitability as cell growth support surfaces, Biomaterials 29 (32) (2008) 4275–4284.
[19] R.S. Cargill Ii, K.C. Dee, S. Malcolm, An assessment of the strength of ng108-15 cell adhesion to chemically modified surfaces, Biomaterials 20 (23–24) (1999) 2417–2425.
[20] A.E. Schaffner, J.L. Barker, D.A. Stenger, J.J. Hickman, Investigation of the factors necessary for growth of hippocampal neurons in a defined system, J. Neurosci. Methods 62 (1–2) (1995) 111–119.
[21] E. Yavin, Z. Yavin, Attachment and culture of dissociated cells from rat embryo cerebral hemispheres on polylysine-coated surface, J. Cell Biol. 62 (2) (1974) 540–546.
[22] Y.H. Kim, N.S. Baek, Y.H. Han, M.-A. Chung, S.-D. Jung, Enhancement of neuronal cell adhesion by covalent binding of poly-d-lysine, J. Neurosci. Methods 202 (1) (2011) 38–44.
[23] T. Elsdale, J. Bard, Collagen substrata for studies on cell behavior, J. Cell Biol. 54 (3) (1972) 626-&.
[24] S. Carbonetto, M.M. Gruver, D.C. Turner, Nerve-fiber growth in culture on fibronectin, collagen, and glycosaminoglycan substrates, J. Neurosci. 3 (11) (1983) 2324–2335.
[25] P.J. Lein, G.A. Banker, D. Higgins, Laminin selectively enhances axonal growth and accelerates the development of polarity by hippocampal neurons in culture. Brain research, Dev. Brain Res. 69 (2) (1992) 191–197.
[26] A. Lochter, M. Schachner, Tenascin and extracellular-matrix glycoproteins — from promotion to polarization of neurite growth in-vitro, J. Neurosci. 13 (9) (1993) 3986–4000.
[27] C.D. James, R. Davis, M. Meyer, A. Turner, S. Turner, G. Withers, L. Kam, G. Banker, H. Craighead, M. Isaacson, J. Turner, W. Shain, Aligned microcontact printing of micrometer-scale poly-l-lysine structures for controlled growth of cultured neurons on planar microelectrode arrays, IEEE Trans. Biomed. Eng. 47 (1) (2000) 17–21.
[28] I. Lieberman, P. Ove, Protein growth factor for mammalian cells in culture, J. Biolumin. Chemilumin. 233 (3) (1958) 637–642.
[29] E.M. Harnett, J. Alderman, T. Wood, The surface energy of various biomaterials coated with adhesion molecules used in cell culture, Colloids Surf. B: Biointerfaces 55 (1) (2007) 90–97.
[30] A. Thalhammer, R.J. Edgington, L.A. Cingolani, R. Schoepfer, R.B. Jackman, The use of nanodiamond monolayer coatings to promote the formation of functional neuronal networks, Biomaterials 31 (8) (2010) 2097–2104.
[31] J.H. Wang, U.H. Lin, C.H. Lin, Y.C. Chung, C.R. Chen, Y.C. Kao, J.Y. Lai, T.H. Young, Change in neuron aggregation and neurite fasciculation on eval membranes modified with different diamines, J. Biomed. Mater. Res. Part A 94A (2) (2010) 489–498.
[32] S.P. Massia, J.A. Hubbell, Immobilized amines and basic-amino-acids as mimetic heparin-binding domains for cell-surface proteoglycan-mediated adhesion, J. Biolumin. Chemilumin. 267 (14) (1992) 10133–10141.
[33] W.L. Gu, S.L. Fu, Y.X. Wang, Y. Li, H.Z. Lu, X.M. Xu, P.H. Lu, Chondroitin sulfate proteoglycans regulate the growth, differentiation and migration of multipotent neural precursor cells through the integrin signaling pathway, BMC Neurosci. 10 (2009) 15.
[34] K.S. Siow, L. Britcher, S. Kumar, H.J. Griesser, Plasma methods for the generation of chemically reactive surfaces for biomolecule immobilization and cell colonization — a review, Plasma Process. Polym. 3 (6–7) (2006) 392–418.
[35] C.D. Hahn, C. Leitner, T. Weinbrenner, R. Schlapak, A. Tinazli, R. Tampé, B. Lackner, C. Steindl, P. Hinterdorfer, H.J. Gruber, M. Hölzl, Self-assembled monolayers with latent aldehydes for protein immobilization, Bioconjug. Chem. 18 (1) (2006) 247–253.
[36] D. Peelen, V. Kodoyianni, J. Lee, T. Zheng, M.R. Shortreed, L.M. Smith, Specific capture of mammalian cells by cell surface receptor binding to ligand immobilized on gold thin films, J. Proteome Res. 5 (7) (2006) 1580–1585.
[37] M.V. Agrez, R.C. Bates, Colorectal-cancer and the integrin family of cell-adhesion receptors — current status and future-directions, Eur. J. Cancer 30A (14) (1994) 2166–2170.
[38] N. Basora, P.H. Vachon, F.E. HerringGillam, N. Perreault, J.F. Beaulieu, Relation between integrin alpha 7b beta 1 expression in human intestinal cells and enterocytic differentiation, Gastroenterology 113 (5) (1997) 1510–1521.